The Journal of Toxicological Sciences (J. Toxicol. Sci.)
Vol.39, No.5, 775-784, 2014

Original Article

Early indicators of delayed adverse effects in female reproductive organs in rats receiving neonatal exposure to 17alpha-ethynylestradiol

Miwa Takahashi[1], Kaoru Inoue[1], Tomomi Morikawa[1], Saori Matsuo[1], Seigo Hayashi[1], Kei Tamura[1], Gen Watanabe[2], Kazuyoshi Taya[2] and Midori Yoshida[1]

[1]Division of Pathology, National Institute of Health Sciences, 1-18-1 Kamiyoga, Setagaya-ku, Tokyo 158-8501, Japan
[2]Laboratory of Veterinary Physiology, Department of Veterinary Medicine, Faculty of Agriculture, Tokyo University of Agriculture and Technology, 3-5-8 Saiwai-cho, Fuchu-shi, Tokyo 183-8509, Japan

(Received May 28, 2014; Accepted August 12, 2014)

ABSTRACT — We previously reported that neonatal exposure to 17α-ethynylestradiol (EE) led to delayed adverse effects in which age-related anovulation after sexual maturation was accelerated. To identify early indicators of these adverse effects, female Wistar Hannover GALAS rats received a single EE injection (0, 0.02, 0.2, 2, 20, or 200 μg/kg) within 24 hr of birth. Histopathological changes in ovarian and uterine development were investigated from postnatal day (PND) 14 to 10 weeks of age. Immunohistochemical expression of estrogen receptor alpha (ERα) in the uterus, serum levels of sex-related hormones and gene expression in the hypothalamus were examined. Although neonatal exposure to EE did not affect body growth or ovarian development, serum FSH tended to decrease at doses ≥ 2 μg/kg, and *Kiss1* mRNA level in the whole hypothalamus was significantly decreased in all EE-treated groups at PND14. The number of uterine glands at PND21 was suppressed at doses ≥ 20 μg/kg, and ERα expression in the uterine epithelium at estrus stage decreased in a dose-dependent manner at 10 weeks of age. These results demonstrated that the various identified changes that occurred before the appearance of delayed adverse effects could be candidate early indicators.

Key words: 17α-ethynylestradiol, Neonatal exposure, Delayed effects, ERα, Rat, Female

INTRODUCTION

In mammals, sexual differentiation of the brain occurs during prenatal and early postnatal development. These organizational processes are critically important for the attainment and maintenance of adult reproductive function (Dickerson *et al*., 2011). The exposure of animals to chemicals with estrogenic activity during the susceptible period of development (late embryonic to early postnatal age in rodents) reportedly causes reproductive deficits (Dickerson *et al*., 2011; Gore *et al*., 2011). In some cases, increased carcinogenic risk and impaired reproductive function are apparent later in life as delayed adverse effects in rodents as well as in humans, even though normal development until maturation (Newbold *et al*., 1990; Newbold, 2011; Swan, 2000).

Previously, we investigated the long-term effects of neonatal exposure to various doses of diethylstilbestrol (DES) or 17α-ethynylestradiol (EE) on the female reproductive tract using rats (Yoshida *et al*., 2011; Takahashi *et al*., 2013). These studies demonstrated that neonatal exposure to DES or EE, which exert estrogenic activity *in vivo*, induced early onset of age-related anovulation in a dose-dependent fashion after sexual maturation. Estrous cyclicity is a precise indicator of delayed adverse effects on the female reproductive tract (Yoshida *et al*., 2011; Takahashi *et al*., 2013). Additionally, it was suggested that the early onset of anovulation leading to prolonged exposure to relatively elevated estrogen might be a risk factor for uterine carcinogenesis. Dysfunction of the ovulation center in the hypothalamus is presumed to be a possible mechanism underlying the early onset of anovulation based on the lack of abnormalities in the remaining follicles and pituitary hormones, although the precise mechanism has not been delineated.

Persistent estrus status resulting from the early onset

Correspondence: Miwa Takahashi (E-mail: mtakahashi@nihs.go.jp)

of anovulation is a useful indicator for delayed effects on female reproductive organs. However, it takes a protracted time to detect the effects caused by neonatal exposure to estrogenic compounds, the onset age being 22 weeks of age at the lowest dose tested (Takahashi *et al.*, 2013). For risk assessment of chemicals, delayed adverse effects have become a serious issue because such effects might be overlooked by existing reproductive toxicity or developmental toxicity studies in accordance with authorized guidelines due to limited observation periods. Thus, toxicologic indicators applicable to early detection of delayed adverse effects are needed for risk assessment of offspring toxicity. The present study was performed to examine early events following neonatal exposure to EE with a view to finding early indicators for subsequent delayed adverse effects. Using rats that received a single EE injection during the neonatal period at doses capable of inducing delayed adverse effects, we conducted histopathological observations of ovarian and uterine development between postnatal day (PND) 14 to 10 weeks of age. In addition, immunohistochemical expression of estrogen receptor alpha (ERα) in the uterus, serum levels of sex-related hormones and gene expression in the whole hypothalamus were examined.

MATERIALS AND METHODS

Animals and chemicals

Pregnant Wistar Hannover GALAS rats (n = 47) were obtained from CLEA Japan, Inc. (Tokyo, Japan) at gestational day 14. The rats were housed individually in polycarbonate cages with wood chip bedding and maintained in an air-conditioned animal room (temperature, 24 ± 1°C; relative humidity, 55 ± 5%) with a basal diet (CRF-1; Oriental Yeast Co., Tokyo, Japan) and tap water available *ad libitum*. Light cycle was set as follows: light on, 5:00-17:00; light off, 17:00-5:00 (12 hr light/dark cycle). The animal protocol was reviewed and approved by the Animal Care and Use Committee of the National Institute of Health Sciences (Japan).

EE was purchased from Sigma (CAS No. 57-63-6; St. Louis, MO, USA) with purity > 98%. EE was stirred in a small amount of sesame oil overnight and then used after dilution.

Experimental design

Dams were assigned to 6 groups before delivery: 2 to 5 dams/group for autopsy at PND14 and 21; 3 to 5 dams/group for autopsy at PND34 and 10 weeks of age. All of the pups received a single subcutaneous injection of EE (0, 0.02, 0.2, 2, 20, or 200 μg/kg of body weight) dissolved in sesame oil (5 mL/kg of body weight) within 24 hr of birth. Litters were culled randomly to preserve 8 pups, with a female predominance on PND3, and then the female offspring were weaned on PND 21 and separated from males. From PND 25, we daily checked the vaginal opening. Estrous cyclicity was continuously monitored by vaginal smear from 7 weeks of age.

On PND 14, 21, and 34, 5 randomly selected female pups per group were autopsied. Additionally, 5 animals at estrus were autopsied at 10 weeks of age. The animals were decapitated, and blood samples were collected for hormone assays. Then, the ovaries, uteri, vagina, adrenals, liver, pituitary, thymus, brain, thyroid, mammary glands and sites with macroscopic abnormalities were removed. At PND34 and 10 weeks of age, weights of the ovaries and uteri were measured. The hypothalamus was dissected out, as described in detail elsewhere (Roa *et al.*, 2006), by a horizontal cut of about 2 mm in depth with the following limits: 1 mm anteriorly from the optic chiasm, the posterior border of mammillary bodies, and the hypothalamic fissures. Hypothalamic samples were immediately removed upon decapitation, frozen in liquid nitrogen, and stored at -80°C until processing for RNA analysis. We excluded 1 animal per group that underwent transcardial perfusion from blood and hypothalamic sampling and measurement of organ weights. The autopsy procedures (including decapitation and blood collection) were conducted in a room separate from the animal room at 10:00 -12:00.

All organs except for the brain were fixed in 10% neutral buffered formalin. Tissues were routinely processed and stained with hematoxylin and eosin (HE) for histopathological examination. The left uterine horns were cut in cross-section at 5 mm intervals. To elucidate the development of uterine glands, the number of uterine glands per section was measured. Using transverse sections of the uterus obtained at PND14, 21 and 34, the number of uterine glands located away from the endometrium was counted, and the number of uterine glands per section per animal was calculated by dividing the number of sections observed. Histological pattern of estrous cycle stage was checked using the ovary, uterus and vagina (Westwood, 2008).

Hormone assays

Serum samples obtained after decapitation were stored at -80°C until assay. The serum concentrations of follicle-stimulating hormone (FSH) and luteinizing hormone (LH) were determined using double-antibody radioimmunoassays and ^{125}I-labeled radio-ligands. National Digestive and Kidney Disease (NIDDK) radioimmunoassay

kits were used for rat FSH and LH (NIAMDD, NIH, Bethesda, MD, USA), as described previously (Taya *et al*., 1983). As for the serum samples at PND34 and 10 weeks of age, estradiol-17β (E2) and progesterone (P4) were measured by radioimmunoassay as described by Taya *et al*. (1985).

Real-time RT-PCR

Total RNA was isolated from whole hypothalamus using ISOGEN II (Nippon Gene Co., Ltd., Tokyo, Japan). Two μg of total RNA was used for reverse transcription (RT) with a high-capacity cDNA Archive Kit (Applied Biosystems Japan Ltd., Tokyo, Japan). Then, quantitative real-time RT-PCR was performed with an ABI Prism 7900HT (Applied Biosystems Japan Ltd.). Taqman® Gene Expression Assay (Applied Biosystems Japan Ltd.) was used to measure mRNA levels of *Kiss1* metastasis-suppressor (*Kiss1*, Rn00710914_m1), KISS1 receptor (*Kiss1r*, Rn00576940_m1), gonadotropin-releasing hormone 1 (*Gnrh1*, Rn00562754_m1), estrogen receptor alpha (*Esr1*, Rn01640372_m1), estrogen receptor beta (*Esr2*, Rn00562610_m1) and cytochrome P450, family 19, subfamily a (aromatase, *Cyp19a1*, Rn00567222_m1). Expression values were normalized to glyceraldehyde 3-phosphate dehydrogenase (*Gapdh*), as *Gapdh* does not change during development in the hypothalamus of rat (Walker *et al*., 2009). The expression level in the 0 μg/kg group was expressed as 1, and relative levels in the EE-treated groups were calculated.

Immunohistochemistry

Formalin-fixed, paraffin-embedded uterine sections (n = 4/group, except for 1 rat that underwent transcardial perfusion) were subjected to immunohistochemistry for ERα and proliferating cell nuclear antigen (PCNA). Rabbit polyclonal antibody against ERα (c-7207, dilution at × 50, Santa Cruz Biotechnology, Inc., Santa Cruz, CA, USA) and mouse monoclonal antibody against PCNA (M0879, dilution at × 100, Dako Japan Inc., Tokyo, Japan) were used as primary antibody (Yoshida *et al*., 2011, 2012). Immunodetection was conducted using Histofine® Simple Stain MAX PO (Nichirei Biosciences Inc., Tokyo, Japan) with 3, 3'-diaminobenzidine/H_2O_2 as the chromogen. For antigen retrieval, the sections were heated in citrate buffer solution (pH 7) by microwave for 10 min at 98°C and 90°C before incubation with the ERα and PCNA antibodies, respectively.

The percentage of ERα and PCNA positive cells was assessed at 400-fold magnification separately in endometrial epithelial cells, uterine glands and stromal cells and scored as follows: 0, negative; 1, slightly positive (< 10%); 2, partly positive (10-30%); 3, positive in about half (30-70%); 4, mostly positive (> 70%). The average score was calculated by observation of 6 randomly selected areas from the upper, middle and lower uterine horns.

Statistical analysis

Because EE was not injected into the dams but into each pup after birth, we analyzed the data by individual pups. A recent report in which pups treated with various doses of EE at PND1 were allocated to foster dams demonstrated that differences between litters have little influence on delayed adverse effect (Shirota *et al*., 2012). However, litter size has a large effect on body growth until sexual maturation. Therefore, the data for body and organ weights were checked by individual pups as well as litters.

Following Bartlett's test, the variance in data for body and organ weights, the number of uterine glands per section, serum hormones, and gene expression levels were compared with the 0 μg/kg group by one-way analysis of variance or the Kruskal-Wallis test. When statistically significant differences were detected, Dunnett's multiple comparison test was employed for comparison between the 0 μg/kg group and the treatment groups.

RESULTS

Body and organ development

Before weaning, no deaths or abnormal clinical signs caused by EE treatment were observed, and body weight gain per animal or per litter was similar among the groups (data not shown). In animals autopsied at PND21, body weight per animals was significantly elevated at 200 μg/kg compared with the 0 μg/kg group (Fig. 1). At PND34, a significant increase of relative brain weight in the 0.02 μg/kg group was found, but without dose-dependency (Table 1). There was no intergroup difference in body or organ weight at 10 weeks of age.

With regard to animals autopsied at PND34 and 10 weeks of age, the average day of vaginal opening was PND30 or 31 (Table 2). No intergroup difference was found when analyzed by individual pups or by litters. As shown in Table 2, although different estrous stage existed at PND34, there was no particular bias among the groups. All animals autopsied at 10 weeks of age demonstrated normal estrous cyclicity in the examination of vaginal smear.

Histopathological examination of the female reproductive organs

In the ovaries, follicular development was normal both

Table 1. Organ weights at postnatal day 34 and 10 weeks of age

		EE (μg/kg)					
		0	0.02	0.2	2	20	200
Postnatal day 34							
No. of animals (No. of litter)		4 (4)	4 (2)	4 (4)	4 (4)	4 (3)	4 (4)
Brain	(g)	1.59 ± 0.02[a]	1.63 ± 0.05	1.62 ± 0.06	1.60 ± 0.10	1.56 ± 0.05	1.62 ± 0.05
	(g/100 g)	1.35 ± 0.01	1.53 ± 0.06 *	1.43 ± 0.10	1.41 ± 0.11	1.37 ± 0.07	1.43 ± 0.07
Ovarica	(mg)	40.0 ± 8.1	33.3 ± 8.0	31.8 ± 0.5	35.8 ± 4.0	37.0 ± 6.2	42.5 ± 5.0
	(mg/100 g)	33.9 ± 6.9	31.0 ± 6.2	28.0 ± 8.4	31.5 ± 1.9	32.6 ± 6.4	37.3 ± 3.7
Uterus	(g)	0.17 ± 0.03	0.16 ± 0.05	0.18 ± 0.09	0.18 ± 0.03	0.26 ± 0.17	0.13 ± 0.02
	(g/100 g)	0.14 ± 0.02	0.15 ± 0.05	0.16 ± 0.08	0.16 ± 0.04	0.23 ± 0.16	0.12 ± 0.01
10 weeks of age							
No. of animals (No. of litter)		4 (4)	4 (4)	4 (4)	4 (4)	4 (3)	4 (4)
Brain	(g)	1.74 ± 0.08	1.76 ± 0.04	1.90 ± 0.10	1.79 ± 0.06	1.80 ± 0.07	1.77 ± 0.07
	(g/100 g)	0.84 ± 0.10	0.78 ± 0.02	0.88 ± 0.05	0.87 ± 0.02	0.82 ± 0.06	0.90 ± 0.10
Ovaries	(mg)	90.0 ± 5.5	92.8 ± 10.6	81.8 ± 14.7	81.0 ± 8.2	82.0 ± 18.3	79.8 ± 13.7
	(mg/100 g)	43.4 ± 2.8	41.0 ± 4.5	37.9 ± 6.4	39.4 ± 4.6	37.6 ± 9.2	39.7 ± 2.1
Uterus	(g)	0.45 ± 0.06	0.51 ± 0.03	0.48 ± 0.06	0.57 ± 0.20	0.65 ± 0.12	0.59 ± 0.41
	(g/100 g)	0.22 ± 0.05	0.23 ± 0.01	0.22 ± 0.02	0.28 ± 0.11	0.29 ± 0.06	0.29 ± 0.20

[a]: mean ± S.D.

*: significantly different from 0 μg/kg group at $p < 0.05$.

Table 2. Mean days of vaginal opening and estrous cycle stage at postnatal day 34 in rats exposed to EE during the neonatal period

EE (μg/kg)	Vaginal opening				Estrous cycle stage at PND34[b]			
	Per animal	(n)	Per litter	(n)	P	E	M	D
0	31.0 ± 0.7 [a]	(10)	31.0 ± 0.6	(5)	0	1	2	2
0.02	31.8 ± 1.4	(10)	31.6 ± 1.3	(7)	2	0	1	2
0.2	30.8 ± 1.1	(10)	30.8 ± 0.9	(5)	0	1	2	2
2	31.3 ± 1.1	(10)	31.3 ± 0.6	(5)	0	2	2	1
20	30.8 ± 0.8	(10)	30.8 ± 0.6	(5)	1	1	3	0
200	30.7 ± 0.8	(10)	30.7 ± 0.7	(5)	0	0	4	1

[a]: mean ± S.D.

[b]: estrous cycle stage was checked by histopathological examination of the ovary, uterus and vagina.

P: proestrus, E: estrus, M: metestrus, D: diestrus

PND, postnatal day.

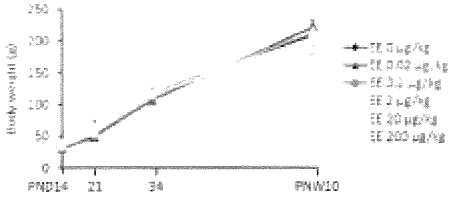

Fig. 1. Body weight curves for rats subjected to neonatal exposure to EE. Data are represent means ± S.D. n = 5 per group. *, significantly different from 0 μg/kg group at $p < 0.05$. PND, postnatal day; PNW, postnatal week.

in the 0 μg/kg and EE-treated groups. Polyovular follicles were evenly found in small number in all groups.

In the 20 and 200 μg/kg groups, the number of uterine glands per section showed a tendency to decrease at PND21 (Fig. 2). At PND34, the number of uterine glands varied widely between individuals. Clear correlation with estrous cycle was not detected and there was no intergroup difference in the number of uterine glands. At 10 weeks of age, significant changes were not seen in the number of uterine glands in the histopathological examination. A few animals from different dams of the 20 and 200 μg/kg group showed some abnormalities in the histology of the ovary, uterus and vagina. Their histology could

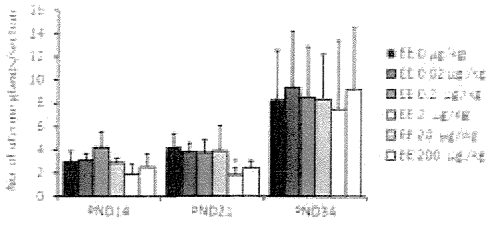

Fig. 2. Number of uterine glands per section from postnatal days 14, 21 and 34. Data represent means ± S.D. n = 5 per group. *: significantly different from 0 μg/kg group at $p < 0.05$.

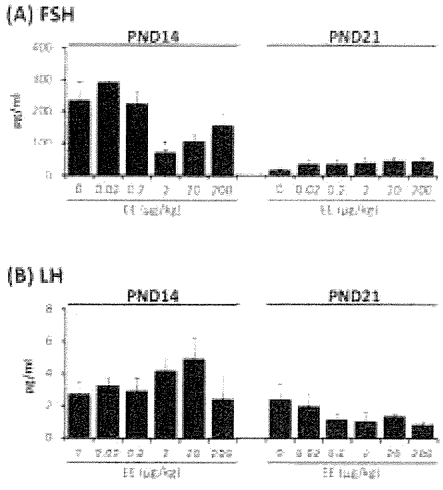

Fig. 3. Serum levels of FSH (A) and LH (B) at postnatal days 14 and 21. Data are means ± S.E. n = 4 per group. *: significantly different from 0 μg/kg group at $p < 0.05$.

not be classified into any estrus cycle stage. In the ovary, newly formed corpora lutea with small basophilic cells, a feature of corpora lutea at estrus, was not found, and the number of recent corpora lutea was decreased. Although there were some large antral follicles, the histology was different from both proestrus and estrus. The lumen of the uterus mildly dilated, and the degeneration/apoptosis of epithelial cells characteristic to estrus was not found. In their vagina, the epithelium showed incomplete keratinization, unlike typical of estrus stage. Treatment-related abnormalities were not found in other organs such as the pituitary, mammary glands, liver, adrenal glands, or the thymus.

Sex-related hormones

The levels of serum FSH and LH at PND14 and 21 are shown in Fig. 3. Serum FSH in the groups treated with 2 μg/kg or more showed a tendency to decrease at PND14. In contrast, the level of LH did not differ among the groups. At PND21, significant changes related to EE treatment were not detected in either FSH or LH. Since the hormone levels widely fluctuated due to mixed estrous stage, intergroup differences were not found in FSH, LH, E2 or P4 at PND34 (data not shown). At 10 weeks of age, level of E2 tended to be high in the animals showing abnormal histology of the ovary, uterus and vagina. The average levels of FSH, LH, E2 or P4 at estrus stage were not statistically different among the groups (Fig. 4).

Expression of Kiss1 and related genes

In the whole hypothalamus, the level of *Kiss1* mRNA was significantly decreased in all of the EE-treated groups at PND14 (Fig. 5). However, *Kiss1* mRNA did not fluctuate at PND21, 34, or 10 weeks of age. No treatment-related change in the expression of *Kiss1r* (Fig. 5), *Esr1*, *Esr2*, *Gnrh* or *Cyp19a1* (data not shown) was found at any time point examined, although a few statistical differences were noted without dose-dependency.

Expression of ERα and PCNA during uterine development

ERα and PCNA were strongly expressed in the nuclei of glandular cells and stromal cells at PND14 in both the 0 μg/kg and the EE-treated groups. Similarly, the expression of ERα or PCNA was mainly found in the glandular cells and stromal cells at PND21 (Fig. 6). Although expression patterns of ERα and PCNA changed depending on the estrous cycle at PND34, there was no difference among the groups. At 10 weeks of age, most of the endometrial epithelial cells expressed ERα in the 0 μg/kg group. In contrast, ERα-positive epithelial cells decreased in a dose-dependent manner, and there were few epithelial cells expressing ERα in the 200 μg/kg group (Fig. 7). The scores for expression of ERα in the glandular cells and stromal cells did not differ among the groups. No intergroup difference was found in the expression of PCNA in the endometrial epithelial cells, uterine glands and strom-

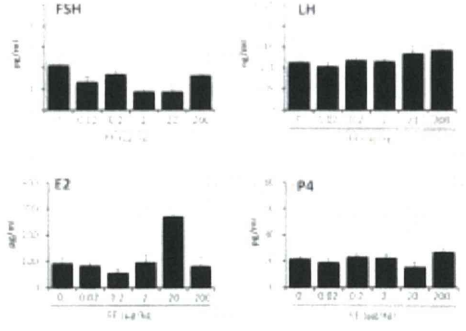

Fig. 4. Serum levels of sex-related hormones at 10 weeks of age. Data are means ± S.E. n = 4 per group.

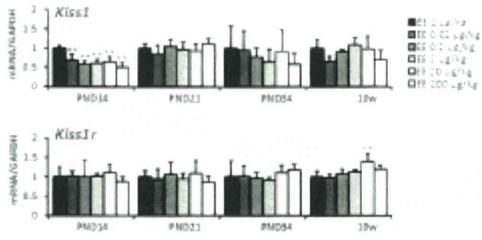

Fig. 5. Hypothalamic mRNA levels of rats subjected to neonatal exposure to EE. Data are means ± S.D. n = 4 per group. **, significantly different from the 0 μg/kg group at p < 0.01.

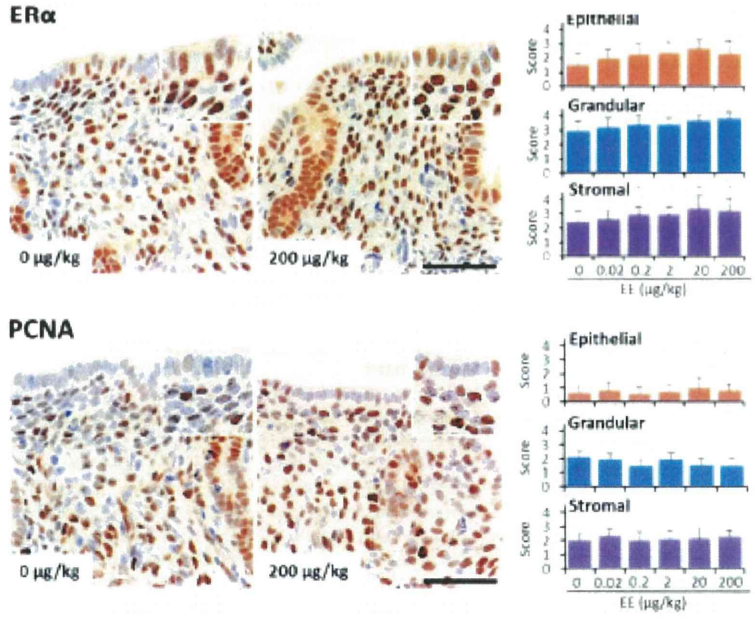

Fig. 6. Immunohistochemical expression of ERα and PCNA in the uterus at postnatal day 21. Representative photomicrographs and scores of positive cells in endometrial epithelial cells, uterine glands and stromal cells. ERα (upper) and PCNA (lower) were strongly expressed in the nuclei of glandular cells and stromal cells both in the 0 μg/kg and EE-treated groups. Upper right corner in each photo shows high-power field of ERα- and PCNA-positive nuclei. Bars = 50 μm. Score: 0, negative; 1, slightly positive (< 10%); 2, partly positive (10-30%); 3, positive in about half (30-70%); 4, mostly positive (> 70%). Data are means + S.D.

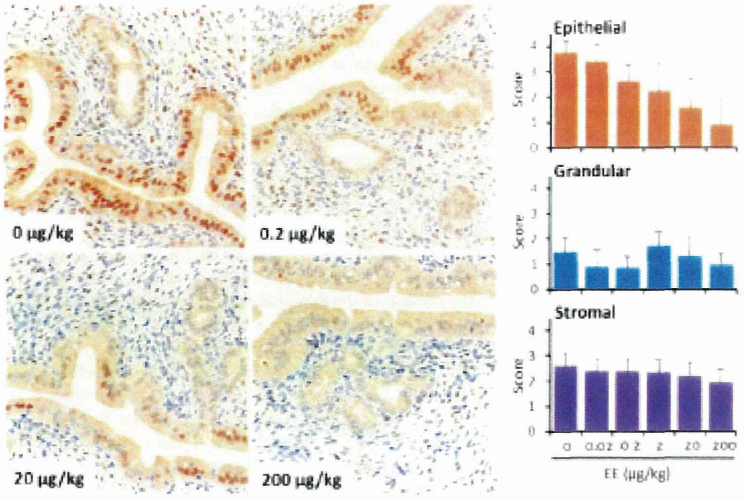

Fig. 7. Immunohistochemical expression of ERα in the uterus at 10 weeks of age. Representative photomicrographs and scores of positive cells in endometrial epithelial cells, uterine glands and stromal cells. In the 0 μg/kg group, most of the endometrial epithelial cells expressed ERα. ERα-positive epithelial cells decreased in a dose-dependent manner and there were few epithelial cells expressing ERα in the 200 μg/kg group. Bars = 50 μm. Score: 0, negative; 1, slightly positive (< 10%); 2, partly positive (10-30%); 3, positive in about half (30-70%); 4, mostly positive (> 70%). Data are means ± S.D.

al cells at 10 weeks of age.

DISCUSSION

A significant increase of body weight was observed in the 200 μg/kg group at PND 21. This finding was considered incidental due to litter size because there were no intergroup differences in the body weight gain of total pups prior to weaning. Although relative brain weight in the 0.02 μg/kg group significantly increased at PND34, it is not regarded as toxicologically significant, because dose-dependency was not found. Therefore, under the present conditions, neonatal exposure to EE did not affect body growth.

In the histopathological examination, there was no effect of EE exposure on ovarian development. It has been reported that the incidence of polyovular follicles was increased by neonatal DES exposure in mice (Iguchi *et al*., 1990). In the present study, polyovular follicles were found in small numbers distributed evenly across all groups, and unrelated to neonatal EE exposure. At 10 weeks of age, although all animals exhibited normal estrous cycle in the examination of the vaginal smear, decrease of recent corpora lutea was observed in a few animals at 20 and 200 μg/kg, suggesting irregular ovulation during recent cycle.

In the uterus, there was a tendency for a decrease in the number of uterine glands per section in the 20 and 200 μg/kg groups at PND21. Additionally, immunohistochemical staining revealed that the expression of ERα by endometrial epithelial cells decreased in a dose-dependent fashion at 10 weeks of age. It is known that early postnatal exposure to estrogenic compounds can suppress uterine gland genesis and expression of estrogen receptors, and can alter the uterine response to estrogen (Branham *et al*., 1985, 1988, Yoshida *et al*., 1999, Katsuda *et al*., 2000, Newbold *et al*., 2004). Therefore, it is likely that these findings were caused by neonatal exposure to EE. Because the doses that showed significant decrease were different between the number of uterine glands at PND21 and the levels of serum FSH and *Kiss1* mRNA at PND14, it is considered that EE directly affected the uterine glands, without through hypothalamus. In our previous study investigating long-term effects

of neonatal exposure to EE (Takahashi *et al*., 2013), the incidence of adenomyosis was decreased in the high dose groups at 10 months of age. Adenomyosis has been reported as a common lesion in aged rats (Dixon *et al*., 1999). It is likely that hormonal perturbations are important for the development of adenomyosis similar to mice, although studies of adenomyosis using rats are very limited (Greaves and White, 2006). Because presence of high P4 level is known to be one of a factor to develop adenomyosis, lowered P4 level at 10 months of age might contribute decreased incidence. However, the possibilities that suppression of uterine gland genesis and alteration of ERα expression affected adenomyosis in later life cannot be excluded. In mice, it has been reported that neonatal exposure to bisphenol A increased adenomyosis (Newbold *et al*., 2007). Therefore, further investigation is required to clarify the early and long-term effects of neonatal exposure to EE on the uterus in rats.

Although incomplete keratinization of vaginal epithelium was observed only in a few animals of the 20 μg/kg group at 10 weeks of age, no abnormality was observed in development or morphology of the vagina in the histopathological examination. In the mammary glands, an increase in acini exhibiting oxyphilic and hypertrophic changes (virilization) was observed at ≥ 0.2 μg/kg in a dose-dependent manner at 10 months of age in our previous report (Takahashi *et al*., 2013). However, treatment-related changes were not found until 10 weeks of age. There are some reports that perinatal exposure to hormonal agents, such as genistein and bisphenol A, leads to abnormal development and morphology of the mammary gland around puberty in rats (Durando *et al*., 2007; El Sheikh Saad *et al*., 2011). Therefore, more detailed examination including quantitative methods might be necessary to clarify whether neonatal exposure to EE affects development of mammary glands or not.

At PND 14, the serum level of FSH exhibited a tendency to decrease at ≥ 2 μg/kg. In rats, the FSH level in blood is low at PND10 and subsequently reaches a peak around PND15, followed by a remarkable reduction at PND25 - 30. This transient increase of FSH occurs independently of inhibin regulation (Herath *et al*., 2001). It has been reported that the peak of FSH is delayed or decreased in androgenized female rats, but the difference disappeared at PND20 - 25 (Cheng and Johnson, 1974; Chiappa and Fink, 1977). Also, chemical exposure during the perinatal period affects the level of FSH in infantile female rats (Wilson and Handa, 1997; Katsuda *et al*., 2000). Therefore, a decrease of FSH level at PND14 might be involved in neonatal EE exposure. However, further study is required to confirm that the peak of FSH is decreased or delayed. On the other hand, there were no intergroup differences in serum hormones at PND34 and 10 weeks of age, although level of E2 tended to be high in the animals showing abnormal histology of the ovary, uterus and vagina at 10 weeks of age. In both our previous and present studies, there was no difference in the average day of vaginal opening (Takahashi *et al*., 2013). Therefore, it is probable that EE exposure in the neonatal period has little impact on ovarian development and sexual maturation.

Dysfunction of the hypothalamus is suspected as one cause of delayed adverse effects (Takahashi *et al*., 2013). Kisspeptin, which is expressed in specific neurons in the anteroventral periventricular (AVPV) nucleus and arcuate (ARC) nucleus of the hypothalamus, is widely recognized as playing a critical role in female reproductive function, including regulation of ovulation and estrous cyclicity (Uenoyama *et al*., 2009; Roa *et al*., 2011). Therefore, we examined the expression of *Kiss1* mRNA in the whole hypothalamus from PND14 to 10 weeks of age. In addition, *Kiss1* related genes such as *Kiss1r*, *Esr1*, *Esr2*, *Gnrh* and *Cyp19a1* were examined using the same samples. Only *Kiss1* showed a significant decrease in all of the EE-treated groups at PND14. Neonatal injection of estradiol benzoate to male and female rats results in a dose-dependent decrease in hypothalamic *Kiss1* mRNA levels in the prepubertal stage (Navarro *et al*., 2009). Therefore, a significant decrease of *Kiss1* mRNA at PND14 might be induced by neonatal exposure to EE. The expression patterns of *Kiss1* in the AVPV and ARC during the postnatal period are different (Takumi *et al*., 2011). At PND14, because the expression level in the ARC is dominant, a decrease of *Kiss1* mRNA is likely to be caused by suppressed expression in the ARC. However, it is known that the AVPV but not the ARC regulates ovulation (Adachi *et al*., 2007). In our study, because we used whole hypothalamus to examine *Kiss1* and its related genes, the expression patterns in the AVPV and ARC were combined. Since the relation between *Kiss1* expression and gonadotropin secretion during postnatal period is not fully understood, the association with the decrease of serum FSH at PND14 or unchanged LH remains uncertain. It is known that the expression levels of *Kiss1* mRNA fluctuates in association with estrous cycle, and its expressions becomes highest in the proestrous afternoon in AVPV to induce LH surge (Adachi *et al*., 2007). The level of *Kiss1* mRNA at PND34 widely fluctuated due to mixed estrous stage in the present study, and further analysis of unified estrous stage will be necessary. In addition to estrus, the expression specific to proestrus should be examined.

In summary, delayed adverse effects have been report-

ed to appear only after maturation so far. However, animals neonatally exposed to EE demonstrated various changes, such as suppressed development of the uterine glands, decreased ERα expression in the uterine epithelium, lowered FSH level, and reduced expression of *Kiss1* mRNA in the hypothalamus prior to the appearance of delayed adverse effects by detailed investigations. Although the association between the above changes and the acceleration of age-related anovulation must be clarified, it is suggested that these changes or their combination might be candidate indicators for the early detection of delayed adverse effects. Particularly, *Kiss1* is expected as the key molecule, because the change was detected from lowest dose and it is directly involved in regulation of ovulation. In order to clarify the relevance between early onset of anovulation and *Kiss1* expression, hypothalamic region and estrous stage specific analysis is currently progress in our laboratory.

ACKNOWLEDGMENTS

We thank Ms. Ayako Saikawa and Yoshimi Komatsu for technical assistance in conducting the animal study. This study was supported by Health and Labour Sciences Research Grants, Research on Risk of Chemical Substances, Ministry of Health, Labour and Welfare, Japan [H22-Toxicol-003].

Conflict of interest---- The authors declare that there is no conflict of interest.

REFERENCES

Adachi, S., Yamada, S., Takatsu, Y., Matsui, H., Kinoshita, M., Takase, K., Sugiura, H., Ohtaki, T., Matsumoto, H., Uenoyama, Y., Tsukamura, H., Inoue, K. and Maeda, K. (2007): Involvement of anteroventral periventricular metastin/kisspeptin neurons in estrogen positive feedback action on luteinizing hormone release in female rats. J. Reprod. Dev., **53**, 367-378.

Branham, W.S., Sheehan, D.M., Zehr, D.R., Ridlon, E. and Nelson, C.J. (1985): The postnatal ontogeny of rat uterine glands and age-related effects of 17 beta-estradiol. Endocrinology, **117**, 2229-2237.

Branham, W.S., Zehr, D.R., Chen, J.J. and Sheehan, D.M. (1988): Uterine abnormalities in rats exposed neonatally to diethylstilbestrol, ethynylestradiol, or clomiphene citrate. Toxicology, **51**, 201-212.

Cheng, H.C. and Johnson, D.C. (1974): Serum estrogens and gonadotropins in developing androgenized and normal female rats. Neuroendocrinology, **13**, 357-365.

Chiappa, S.A. and Fink, G. (1977): Releasing factor and hormonal changes in the hypothalamic-pituitary-gonadotrophin and -adrenocorticotrophin systems before and after birth and puberty in male, female and androgenized female rats. J. Endocrinol., **72**, 211-224.

Deckersen, S.M., Cunningham, S.L., Patisaul, H.B., Woller, M.J. and Gore, A.C. (2011): Endocrine disruption of brain sexual differentiation by developmental PCB exposure. Endocrinology, **152**, 581-594.

Dixon, D., Leininger, J.R., Valerio, M.G., Johnson, A.N., Stalinski, L.G. and Frith, C.H. (1999): Proliferative lesions of the ovary, uterus, vagina, cervix and oviduct in rats. URG-5. In Guides for Toxicologic Pathology, STP ARP AFIP, Washington, DC.

Durando, M., Kass, L., Piva, J., Sonnenschein, C., Soto, A.M., Luque, E.H. and Muñoz-de-Toro, M. (2007): Prenatal bisphenol A exposure induces preneoplastic lesions in the mammary gland in Wistar rats. Environ. Health Perspect., **115**, 80-86.

El Sheikh Saad, H., Meduri, G., Phrakonkham, P., Bergès, R., Vacher, S., Djallali, M., Auger, J., Canivenc-Lavier, M.C. and Perrot-Applanat, M. (2011): Abnormal peripubertal development of the rat mammary gland following exposure in utero and during lactation to a mixture of genistein and the food contaminant vinclozolin. Reprod. Toxicol., **32**, 15-25.

Gore, A.C., Walker, D.M., Zama, A.M., Armenti, A.E. and Uzumcu, M. (2011): Early life exposure to endocrine-disrupting chemicals causes lifelong molecular reprogramming of the hypothalamus and premature reproductive aging. Mol. Endocrinol., **25**, 2157-2168.

Greaves, P. and White, I.N. (2006): Experimental adenomyosis. Best Pract. Res. Clin. Obstet. Gynaecol., **20**, 503-510.

Heram, C.B., Yamamura, M., Watanabe, G., Jin, W., Taneyamagup, S., Kojima, A., Greenne, N.P., Suzuki, A.K. and Taya, K. (2001): Regulation of follicle-stimulating hormone secretion by estradiol and dimeric inhibins in the infantile female rat. Biol. Reprod., **65**, 1623-1633.

Iguchi, T., Fukazawa, Y., Uesugi, Y. and Takasugi, N. (1990): Polyovular follicles in mouse ovaries exposed neonatally to diethylstilbestrol *in vivo* and *in vitro*. Biol. Reprod., **43**, 478-484.

Katsuda, S., Yoshida, M., Watanabe, G., Taya, K. and Maekawa, A. (2000): Irreversible effects of neonatal exposure to p-tert-octylphenol on the reproductive tract in female rats. Toxicol. Appl. Pharmacol., **165**, 217-226.

Navarro, V.M., Sánchez-Garrido, M.A., Castellano, J.M., Roa, J., García-Galiano, D., Pineda, R., Aguilar, E., Pinilla, L. and Tena-Sempere, M. (2009): Persistent impairment of hypothalamic KiSS-1 system after exposures to estrogenic compounds at critical periods of brain sex differentiation. Endocrinology, **150**, 2359-2367.

Newbold, R.R., Bullock, B.C. and McLachlan, J.A. (1990): Uterine adenocarcinoma in mice following developmental treatment with estrogens: a model for hormonal carcinogenesis. Cancer Res., **50**, 7677-7681.

Newbold, R.R., Jefferson, W.N., Padilla-Banks, E. and Haseman, J. (2004): Developmental exposure to diethylstilbestrol (DES) alters uterine response to estrogens in prepubescent mice: low versus high dose effects. Reprod. Toxicol., **18**, 399-406.

Newbold, R.R., Jefferson, W.N. and Padilla-Banks, E. (2007): Long-term adverse effects of neonatal exposure to bisphenol A on the murine female reproductive tract. Reprod. Toxicol., **24**, 253-258.

Newbold, R.R. (2011): Developmental exposure to endocrine-disrupting chemicals programs for reproductive tract alterations and obesity later in life. Am. J. Clin. Nutr., **94**, 1939S-1942S.

Roa, J., Navarro, V.M. and Tena-Sempere, M. (2011): Kisspeptins in reproductive biology: consensus knowledge and recent developments. Biol. Reprod., **85**, 650-660.

Roa, J., Vigo, E., Castellano, J.M., Navarro, V.M., Fernández-Fernández, R., Casanueva, F.F., Dieguez, C., Aguilar, E.,

Pinilla, L. and Tena-Sempere, M. (2006): Hypothalamic expression of KiSS-1 system and gonadotropin-releasing effects of kisspeptin in different reproductive states of the female Rat. Endocrinology, **147**, 2864-2878.

Shiorta, M., Kawashima, J., Nakamura, T., Ogawa, Y., Kamite, J., Yasuno, K., Shirota, K. and Yoshida, M. (2012): Delayed effects of single neonatal subcutaneous exposure of low-dose 17α-ethynylestradiol on reproductive function in female rats. J. Toxicol. Sci., **37**, 681-690.

Swan, S.H. (2000): Intrauterine exposure to diethylstilbestrol: long-term effects in humans. APMIS, **108**, 793-804.

Takahashi, M., Inoue, K., Morikawa, T., Matsuo, S., Hayashi, S., Tamura, K., Watanabe, G., Taya, K. and Yoshida, M. (2013): Delayed effects of neonatal exposure to 17alpha-ethynylestradiol on the estrous cycle and uterine carcinogenesis in Wistar Hannover GALAS rats. Reprod. Toxicol., **40**, 16-23.

Takumi, K., Iijima, N. and Ozawa, H. (2011): Developmental changes in the expression of kisspeptin mRNA in rat hypothalamus. J. Mol. Neurosci., **43**, 138-145.

Taya, K., Mizokawa, T., Matsui, T. and Sasamoto, S. (1983): Induction of superovulation in prepubertal female rats by anterior pituitary transplants. J. Reprod. Fertil., **69**, 265-270.

Taya, K., Watanabe, G. and Sasamoto, S. (1985): Radioimmunoassay for progesterone, testosterone, and estradiol-17β using 125I-iodohistamine radioligands. Jpn. J. Anim. Reprod., **31**, 186-197.

Uenoyama, Y., Tsukamura, H. and Maeda, K.I. (2009): Kisspeptin metastin: a key molecule controlling two modes of gonadotrophin-releasing hormone luteinising hormone release in female rats. J. Neuroendocrinol., **21**, 299-304.

Walker, D.M., Juenger, T.E. and Gore, A.C. (2009): Developmental profiles of neuroendocrine gene expression in the preoptic area of male rats. Endocrinology, **150**, 2308-2316.

Westwood, F.R. (2008): The female rat reproductive cycle: a practical histological guide to staging. Toxicol. Pathol., **36**, 375-384.

Wilson, M.E. and Handa, R.J. (1997): Gonadotropin secretion in infantile rats exposed to ethanol in utero. Alcohol, **14**, 497-501.

Yoshida, A., Newbold, R.R. and Dixon, D. (1999): Effects of neonatal diethylstilbestrol (DES) exposure on morphology and growth patterns of endometrial epithelial cells in CD-1 mice. Toxicol. Pathol., **27**, 325-333.

Yoshida, M., Takahashi, M., Inoue, K., Hayashi, S., Maekawa, A. and Nishikawa, A. (2011): Delayed adverse effects of neonatal exposure to diethylstilbestrol and their dose dependency in female rats. Toxicol. Pathol., **39**, 823-834.

Yoshida, M., Katsuda, S. and Maekawa, A. (2012): Involvements of Estrogen Receptor, Proliferating Cell Nuclear Antigen and p53 in Endometrial Adenocarcinoma Development in Donryu Rats. J. Toxicol. Pathol., **25**, 241-247.

Toxicologic Pathology, 42: 1174–1187, 2014

ISSN: 0192-6233 print / 1533-1601 online
DOI: 10.1177/0192623314530194

Inhibitory Potential of Postnatal Treatment with Cyclopamine, a Hedgehog Signaling Inhibitor, on Medulloblastoma Development in Ptch1 Heterozygous Mice

Saori Matsuo[1,2], Miwa Takahashi[1], Kaoru Inoue[1], Kei Tamura[1], Kaoru Irie[1], Yukio Kodama[3], Akiyoshi Nishikawa[2,4], and Midori Yoshida[1]

[1]*Division of Pathology, National Institute of Health Sciences, Tokyo, Japan*
[2]*Pathogenetic Veterinary Science, United Graduate School of Veterinary Sciences, Gifu University, Gifu, Japan*
[3]*Division of Toxicology, National Institute of Health Sciences, Tokyo, Japan*
[4]*Biological Safety Research Center, National Institute of Health Sciences, Tokyo, Japan*

Abstract

Medulloblastomas (MBs) are thought to be derived from granular cell precursors in the external granular layer (EGL) of the developing cerebellum. Heterozygous patched1 (Ptch1) knockout mice develop MBs that resemble those in humans when the sonic hedgehog (Shh) signaling pathway is activated. The present study was conducted to evaluate postnatal effects of a Shh signaling inhibitor, cyclopamine, on the development of MBs in Ptch1 mice. Ptch1 and wild-type mice were treated daily with subcutaneous cyclopamine at 40 mg/kg or vehicle from postnatal day (PND) 1 to PND14, and the subsequent development of MBs and preneoplastic lesions was examined up to week 12 (W12). Proliferative lesions in the cerebellum, MBs, and preneoplastic lesions were only detected in Ptch1 mice. Cyclopamine treatment resulted in a statistically significant reduction in the incidence and/or area of proliferative lesions at PND14 and 21. The trend of decreasing preneoplastic lesions persisted up to W12. At PND7, cyclopamine treatment reduced the width and proliferation of the EGL regardless of genotype. These results indicate that inhibition of Shh signaling during cerebellar development has prolonged inhibitory potential on MB development in Ptch1 mice. This inhibitory potential might be related to inhibition of EGL proliferation, including preneoplastic MB cells.

Keywords: cyclopamine; cerebellum; medulloblastoma; patched1; preneoplastic lesion; smoothened inhibitor; sonic hedgehog inhibitor.

Introduction

Medulloblastoma (MB) is the most common malignant brain tumor in children (Bartlett, Kortmann, and Saran 2013; Dhall 2009; Hatten and Roussel 2011; Jones et al. 2012). Although exposure to environmental compounds and radiation during the developmental period and early life stages has been thought to be critically involved in the causation of tumors, little is known about the etiology of childhood brain tumors (Bunin et al. 2006; Birnbaum and Fenton 2003; Dietrich et al. 2005; Mckean-Cowdin et al. 2003; Norman, Holly, and Preston-Martin 1996; Takahashi et al. 2012).

Molecular analysis of sporadic human MBs revealed activation of the sonic hedgehog (Shh) signaling pathway caused by the loss of *patched1* (*Ptch1*) and mutations in other components of the Shh pathway. *Ptch1* encodes a receptor for Shh, Ptch1, and is one of the key genes related to MB formation in humans (Dhall 2009; Raffel 2004). Pathway activation is triggered by binding of Shh to Ptch1; in the absence of Shh, the activity of Smoothened (Smo) is suppressed. Shh binding to Ptch1 or mutational inactivation of Ptch1 relieves the inhibition on Smo culminating in the activation of one or more of the Gli1 transcription factors that regulate the expression of downstream targets (Hahn et al. 1999; Huse and Holland 2010; Roussel and Hatten 2011).

Heterozygous *Ptch1* knockout mice (Ptch1 mice) have been used as a valuable model of MB due to the high incidence of MBs (14–30%) and the morphological and molecular similarities to human MBs (Corcoran and Scott 2001; Goodrich et al. 1997; Hahn et al. 1999; Pazzaglia 2006; Raffel 2004; Wetmore, Eberhart, and Curran 2000). Moreover, it has been reported that Shh signaling is activated in MBs of Ptch1 mice (Dyer 2004; Goodrich et al. 1997; Oliver et al. 2005; Wetmore, Eberhart, and Curran 2000).

MBs in humans and Ptch1 mice are thought to be derived from residual granule cell precursors (GCPs) located in the external granule cell or external granular (germinal) layer (EGL) of the cerebellum (Behesti and Marino 2009; Roussel

The author(s) declared no potential conflicts of interest with respect to the research, authorship, and/or publication of this article.

The author(s) disclosed receipt of the following financial support for the research, authorship, and/or publication of this article: This study was partly supported by Health and Labor Sciences Research Grants, Research on Risk of Chemical Substances, Ministry of Health, Labor and Welfare [H25-Toxicol-003].

Address correspondence to: M. Yoshida, Division of Pathology, National Institute of Health Sciences, 1-18-1 Kamiyoga, Setagaya-ku, Tokyo 158-8501, Japan; e-mail: midoriy@nihs.go.jp.

Abbreviations: EGL, external granular layer; GCP, granule cell precursor; HGF, hepatocyte growth factor; MB, medulloblastoma; PND, postnatal day; Ptch1, patched1; Shh, sonic hedgehog; Smo, smoothened; W12, postnatal week 12.

and Hatten 2011). During normal cerebellar development in mice, GCPs proliferate postnatally, and the proliferative period peaks between postnatal days (PND) 4 and 8 (Behesti and Marino 2009; Roussel and Hatten 2011). For GCP proliferation, Shh signaling is required (Lewis et al. 2004; Raffel 2004; Roussel and Hatten 2011; Vaillant and Monard 2009; Wallace 1999).

While Ptch1 mice have been accepted as a useful MB model, it takes an extended amount of time to detect the efficacy of treatments using end points such as the clinical signs of increased intracranial pressure due to MB or death after the long latent period of 9 to over 12 months (Ayrault et al. 2009; Briggs et al. 2008; Ecke et al. 2008; Farioli-Vecchioli et al. 2007; Kimura et al. 2005; Pazzaglia et al. 2006; Pazzaglia et al. 2009; Pogoriler et al. 2006; Uziel et al. 2005; Wetmore, Eberhart, and Curran 2001).

Recently, we found that the earliest signs of MBs and their preneoplastic lesions in Ptch1 mice were morphologically detectable within 2 weeks after birth (Matsuo et al. 2013). Changes in these indicators are thought to be early novel end points for assessment of the modifying effects of chemicals and/or agents on MB development in studies using Ptch1 mice.

Cyclopamine is a naturally occurring alkaloid of the corn lily *Veratrum californicum* that causes cyclopia in sheep by blocking the Shh/Ptc/Smo signaling pathway (Ecke et al. 2008; Heretsch et al. 2010a and b; Lipinski et al. 2008). The inhibitory effects of cyclopamine on the Shh pathway have been reported in a number of *in vitro* and *in vivo* studies (Ecke et al. 2008; Scales and Sauvage 2009; Stecca and Ruiz i Altaba 2002). Furthermore, cyclopamine was shown to inhibit the *in vitro* growth of human MB cell lines (Berman et al. 2002), and other studies have examined the effect of cyclopamine *in vivo* on spontaneously developing Hedgehog (Hh)-dependent tumors including MBs (Sanchez and Ruiz i Altaba 2005; Ecke et al. 2008; Fan et al. 2011; Coon et al. 2010). However, the effects of developmental exposure to cyclopamine using Ptch1 mice have not been reported. Here, we used the Ptch1 mouse model of MB to test if cyclopamine treatment from PND 1 to 14 is able to inhibit tumor growth and to affect cerebellar development.

Materials and Methods

Animals

Heterozygous ptch1 knockout mice (Ptch1 mice) maintained on a mixed C57Bl/6 × 129Sv background were obtained from the Jackson Laboratory (Bar Harbor, ME). Mice were housed in our facility in polycarbonate cages with wood chip bedding and maintained in an air-conditioned animal room (temperature 24°C ± 1°C, relative humidity 55% ± 5%, 12-hr light–dark cycle) with a basal diet (CRF-1, Oriental Yeast Co., Tokyo, Japan) and tap water available *ad libitum*. Animals were genotyped by polymerase chain reaction amplification of genomic DNA extracted from tails (Matsuo et al. 2013). The experimental protocol regarding animal use was reviewed and approved by the Animal Care and Use Committee of the National Institute of Health Sciences, Japan.

Cyclopamine Treatment

Cyclopamine (CAS No. 4449-51-8, purity >99%, LC Laboratories, Woburn, MA) was dissolved in ethanol then suspended in triolein (Wako, Osaka, Japan). Animals were weighed just prior to each injection, and cyclopamine (40 mg/kg/day) or vehicle (triolein: ethanol, 4:1 vol/vol) was injected subcutaneously from PND1 to PND14. The dosing volume, dose of cyclopamine and vehicle, and route of administration were selected based on previous studies (Berman et al. 2002; Lipinski et al. 2008) and our preliminary study. The administration period, from PND1 to PND14, was chosen to match the developmental period in the cerebellum in which GCP proliferation is prominent (Behesti and Marino 2009; Haldipur et al. 2012; Vaillant and Monard 2009). This duration also covers the highly susceptible period of Ptch1 mice to X-ray irradiation and carcinogens (Pazzaglia et al. 2002; Takahashi et al. 2012). The number of mice in each group at each time point is listed in Table 1. At least 5 wild-type mice and 9 Ptch1 mice from 3 to 9 dams were allocated to each group.

Necropsy

To examine the effects of cyclopamine on early cerebellar development, Ptch1 and wild-type mice at PND7 were subjected to necropsies. To examine the effect of cyclopamine on MB development, necropsy was performed at PND14 and PND21. In addition, at postnatal week 12 (W12), Ptch1 and wild-type mice were examined to determine whether the effects of cyclopamine treatment on the cerebellum during the developmental period persist after the maturation of the cerebellum. At necropsy, all mice were euthanized under deep anesthesia with isoflurane.

Tissue Processing and Histopathology

After necropsy, brains were removed and weighed before fixation in 10% neutral buffered formalin. Midsagittal (right hemisphere) and cross (left hemisphere) sections of the cerebella were routinely processed for paraffin embedding, sectioned, and stained with hematoxylin and eosin. The prepared histopathological specimens were examined by light microscopy. To examine the effect of cyclopamine on MB development, we counted preneoplastic lesions such as thickenings of the EGL at PND14 and Ki-67-positive foci at PND21 and W12 in addition to MBs. MBs were divided into 2 types according to the previous study (Matsuo et al. 2013): a focal MB occupying 1 to 2 lobules of the cerebellum was defined as a small MB and an advanced MB spreading over 3 or more lobules was defined as a large MB.

Immunohistochemistry

Antibodies used for immunohistochemistry included monoclonal rat anti-mouse Ki-67 (Clone TEC-3, Dako Cytomation,

TABLE 1.—Body weight, brain weight, and cerebellum weight.

	PND7				PND14				PND21			
	Control		Cyclopamine		Control		Cyclopamine		Control		Cyclopamine	
	Wild	Ptch1	Wild	Ptch1	Wild	Ptch1	Wild	Ptch1	Wild	Ptch1	Wild	Ptch1
n	8	12	7	17	6	12	9	9	6	17	7	18
Body weight (g)	4.4 ± 0.9	3.9 ± 0.8	3.8 ± 0.2	3.6 ± 0.6	6.6 ± 0.4	6.5 ± 1.0	6.1 ± 1.6	6.5 ± 1.3	9.4 ± 1.5	9.7 ± 1.5	9.7 ± 1.7	9.2 ± 1.7
Brain weight (mg)	243 ± 17	256 ± 12	228 ± 11	238 ± 19**	341 ± 16	379 ± 19	324 ± 26	363 ± 21	417 ± 29	453 ± 18	366 ± 16**	410 ± 25**
Cerebellum weight (mg)	64 ± 6	74 ± 6	61 ± 4	66 ± 6**	94 ± 5	108 ± 5	90 ± 8	106 ± 11	115 ± 8	133 ± 9	102 ± 3**	119 ± 10**

Note. PND = postnatal day; Ptch1 = patched1.
**Significantly different from control group at $p < .01$.

Glostrup, Denmark) as a proliferation marker, monoclonal rabbit anti-cleaved caspase-3 (Clone 5A1E, Cell Signaling, Danvers, MA) as an apoptotic marker, and monoclonal mouse anti-NeuN (Clone A60, Millipore, Billerica, MA) as a mature granule cell marker. A streptavidin–biotin labeling method was performed with the anti-Ki-67 antibody using a polyclonal rabbit anti-rat biotinylated IgG (Dako Cytomation) and streptavidin-conjugated horseradish peroxidase (Dako Cytomation). A polymer labeling method was performed for the anti-cleaved caspase-3 and anti-NeuN antibodies using the Histofine Simple Stain kit (Nichirei Biosciences Inc., Tokyo, Japan). The immunoreactions were visualized by a peroxidase-diaminobenzidine reaction. The sections were then lightly counterstained with hematoxylin.

Morphometric Assessment

For total area of proliferative lesions in the cerebellum, photomicrographs of the cerebellar sections were taken with a digital camera attached to a microscope (DP71, Olympus Corp., Tokyo, Japan), then measurements were made using image analysis software (WinROOF, Version 5.7.1, Mitani Corp., Tokyo, Japan). The total area of proliferating cells in the cerebellum, including Ki-67-positive foci and MBs (Matsuo et al. 2013), was measured as the Ki-67-positive cell area, and the ratio of the total proliferating area to the total area of the cerebellum was calculated for Ptch1 mice at PND21 and W12. For width of the EGL and outer layer of EGL, slides stained with Ki-67 antibody were scanned using Aperio ScanScope (Aperio, Vista, CA), then measurements were made using image analysis software (ImageScope, Version 10.2.1.2315, Aperio, Vista, CA). The width of the EGL and the outer layer of the EGL of each mouse at PND7 was determined by 5 measurements selected at random from the 3rd cerebellar lobule.

Statistical Analysis

For body weight, organ weight, proliferating area of the cerebellum, and width of the EGL and outer layer of the EGL, values of cyclopamine-treated mice at each time point were compared with the corresponding vehicle controls using the Student's *t*-test following a test for equal variance. Incidence of histopathological findings was compared using Fisher's exact probability test.

Results

General Remarks

There were no significant differences in body weight at each time point when control and cyclopamine-treated mice were compared by genotype (Table 1). All wild-type and Ptch1 mice survived the duration of the experimental period. In addition, no clinical signs of tumor progression were detected in either genotype with or without cyclopamine treatment up to 12 weeks of age.

Absolute weights of the whole brain and cerebellum significantly decreased in Ptch1 mice in the cyclopamine group at PND7, and in both genotypes in the cyclopamine group at PND21 compared to the control group (Table 1).

Effect of Cyclopamine on Proliferative Lesions in the Cerebellum of Ptch1 Mice

No proliferative lesions were detected in the cerebellum of wild-type mice at any time point (Figure 1). The incidence of lesions was calculated as the number of animals that had a specific lesion (e.g., Ki-67-positive foci) in the cerebellum relative to the total number of animals examined (Figures 2 and 3). At PND14, the incidence of thickened areas in the EGL was significantly decreased in the cyclopamine group in Ptch1 mice (Figure 3). In addition, the incidence of Ki-67-positive foci and small MBs was significantly decreased in the cyclopamine group in Ptch1 mice at PND21 (Figure 3). The incidence of proliferative lesions in the cerebellum of the cyclopamine group in Ptch1 mice at W12 was decreased but was not statistically significant (Figure 3).

Immunohistochemistry for Ki-67 revealed that the total area of proliferative lesions in the cerebellum was significantly decreased in the cyclopamine group in Ptch1 mice at PND21 (Figure 4). Additionally, a decreasing trend in the total area of proliferative lesions at W12 was observed (Figure 4).

Effects of Cyclopamine on Cerebellar Development

To examine the specific inhibitory effects of cyclopamine on the development of MBs and their preneoplastic lesions, we also performed histopathology of the cerebellum of control and cyclopamine-treated mice during the early developmental period of the cerebellum at PND7. The width of the EGL was noticeably thinned in the cyclopamine group compared to the control group regardless of genotype at PND7 (Figures 5A and 6, pictures of wild-type mice not shown). The thinning of the EGL was mainly observed in lobules 2 through 4/5 of the cerebellum and was obscure in lobules 6 through 10. Immunohistochemical staining with the anti-Ki-67 antibody revealed that the outer layer of the EGL, which is composed of proliferating GCPs, was also thinned in Ptch1 mice in the cyclopamine group (Figures 5B and 6, pictures of wild-type mice not shown). Decreasing trend was observed in the outer layer of the EGL in cyclopamine group of wild-type mice (Figure 5B). There was no increase in cleaved caspase-3-positive apoptotic cells in the EGL of the cyclopamine group compared to the control group (Figure 6).

Histopathological examination revealed that cells morphologically resembling nuclei of the internal granular layer were distributed parallel to the Purkinje cell layer in the deep molecular layer of the cyclopamine group at PND14 and 21 regardless of genotype (Figure 7). These nuclei were strongly labeled for NeuN (Figure 8). These findings were also present in the cerebellum of the cyclopamine-treated group at W12 (Figures 7 and 8). Furthermore, misalignment of the Purkinje cells was

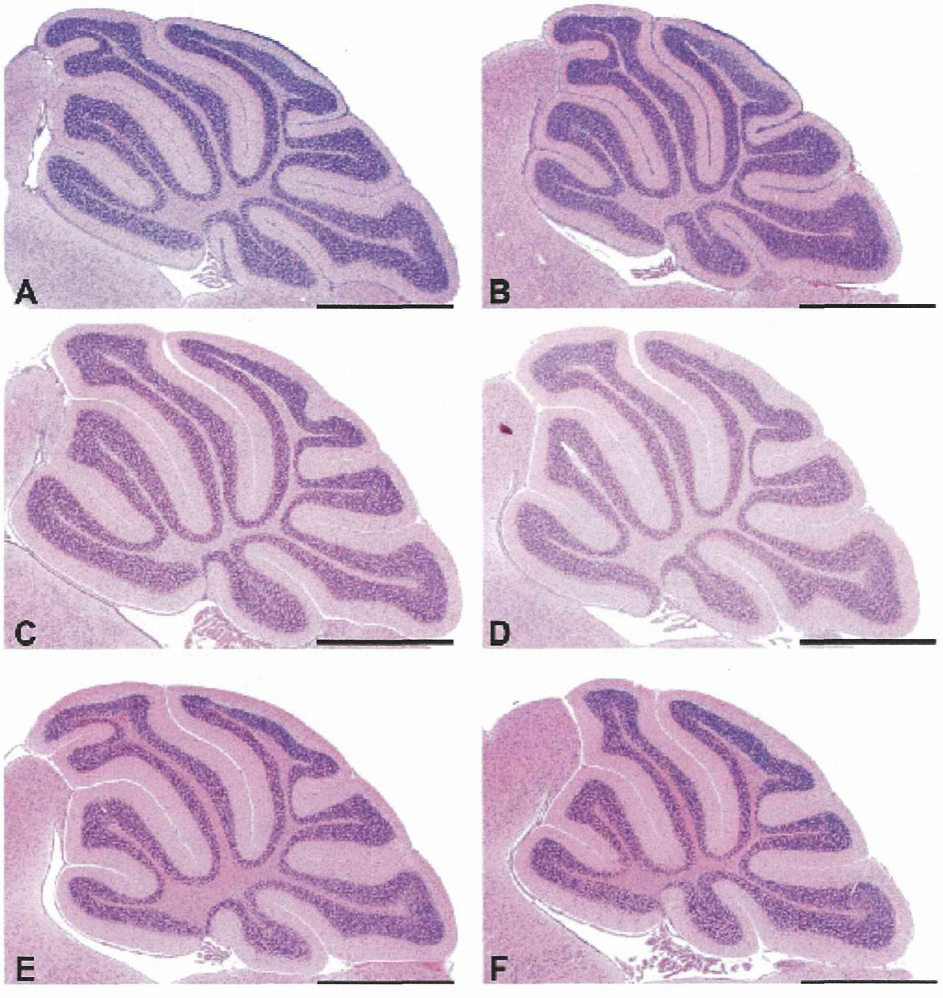

FIGURE 1.—Representative images of the cerebellum from control (left) and cyclopamine-treated (right) wild-type mice at PND14 (A, B), 21 (C, D) and W12 (E, F). No proliferative lesions were detected in the cerebellum of wild-type mice at any time point. Scale bar: 1000 μm.
Note. PND = postnatal day; W12 = postnatal week 12.

scattered in the cyclopamine group at PND14 and 21, and this finding was observed up to W12 (Figure 9). These findings were mainly observed in lobules 2 through 4/5 of the cerebellum and were obscure in lobules 6 through 10 in both genotypes (pictures of wild type not shown).

DISCUSSION

Currently, human MBs have been classified into at least 4 distinct subtypes by molecular studies (Ellison et al. 2011; Northcott et al. 2011; Jones et al. 2012; Kool et al. 2012; Kawauchi et al. 2012). MBs of the Shh subgroup result from

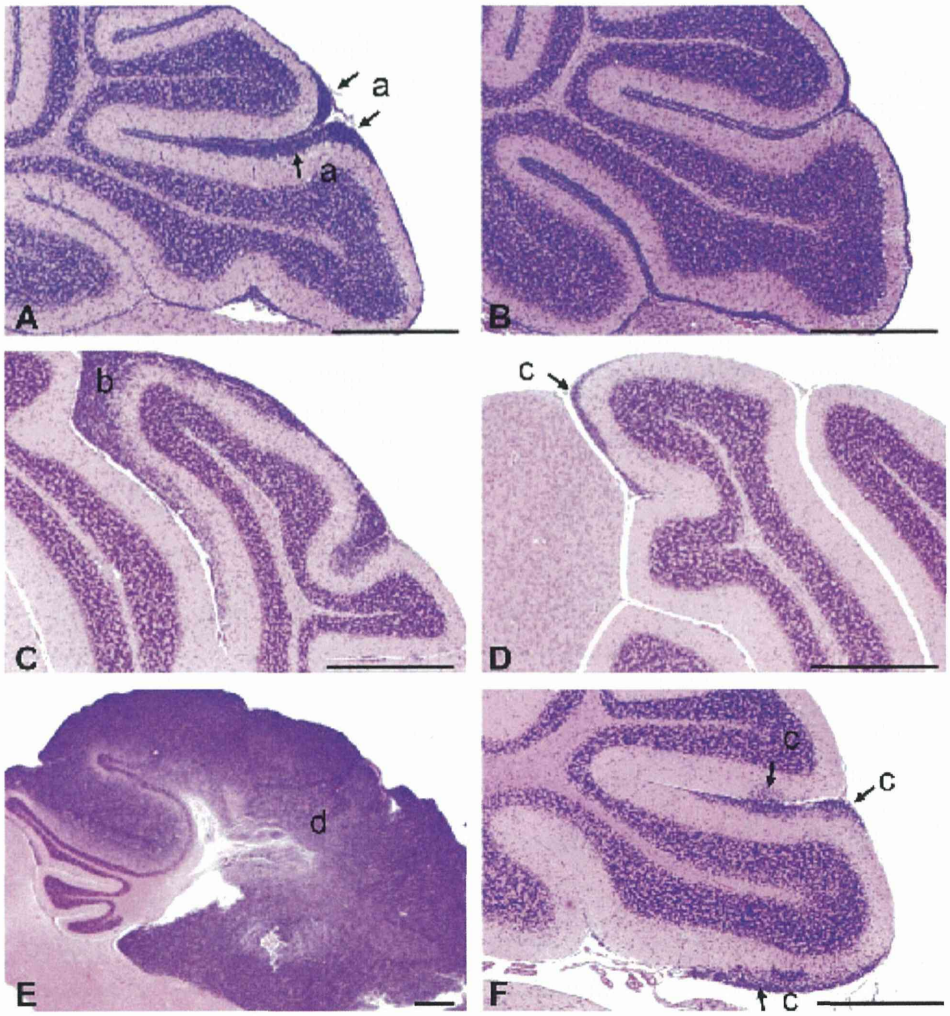

FIGURE 2.—Representative proliferative lesions in the cerebellum of control (left) and cyclopamine-treated (right) Ptch1 mice at PND14 (A, B), 21 (C, D) and W12 (E, F). Proliferative lesions in the cerebellum were classified into the following 4 types: (a) thickened area of the EGL, (b) small MB, (c) Ki-67 positive focus, and (d) large MB. Scale bar: 500 μm.
Note. PND = postnatal day; W12 = postnatal week 12; Ptch1 = patched1; EGL = external granular layer; MB = medulloblastoma.

inactivating mutations of PTCH1 or mutations of other components of the Shh signaling pathway (Kawauchi et al. 2012). It is known that the expression of Gli1 is increased in MBs of Ptch1 mice compared to expression in the normal cerebellum, suggesting activation of the Shh signaling pathway in these tumors (Raffel 2004). Recently, many Shh pathway inhibitors such as cyclopamine, HhAntag, GDC-0449, and IPI-926 have been identified and tested in preclinical and clinical studies

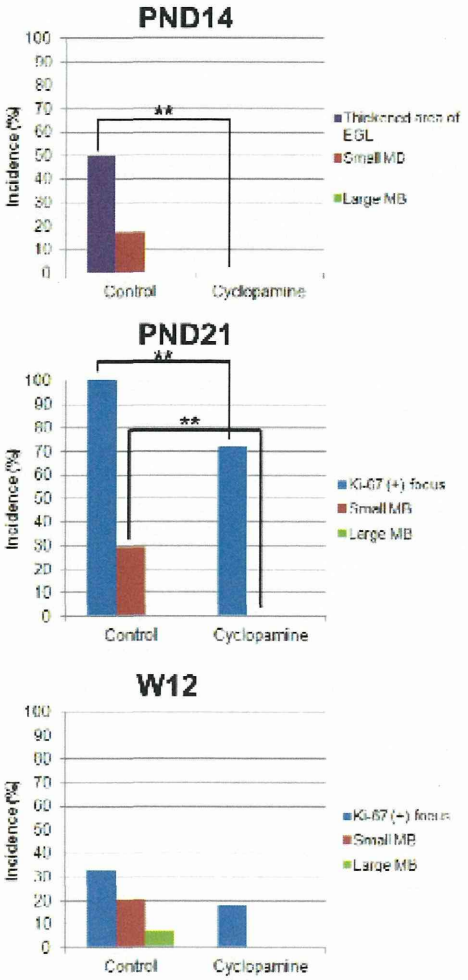

FIGURE 3.—Incidence of proliferative lesions in the cerebellum of control and cyclopamine-treated Ptch1 mice at PND14, 21, and W12. **Significantly different from control group; $p < .01$.
Note. PND = postnatal day; W12 = postnatal week 12; Ptch1 = patched1.

targeting MB and other Shh pathway–activated tumors (Gajjar et al. 2013; Gupta, Takebe, and Lorusso 2010; Lee et al. 2012; Low and Sauvage 2010; Scales and Sauvage 2009). The Ptch1 mouse has been used in various studies as an Shh-subtype MB model (Behesti and Marino 2009; Sanchez and Ruiz i Altaba 2005).

During postnatal cerebellar development in mice, proliferation of GCPs occurs throughout the 2 weeks after birth and GCPs migrate into the internal granular layer by PND21 (Behesti and Marino 2009; Haldipur et al. 2012; Vaillant and Monard 2009). During postnatal cerebellar development, Ptch1 mice show a high incidence of preneoplastic MB lesions such as thickened areas in the EGL and Ki-67 positive foci (Matsuo et al. 2013). The present study clearly showed that postnatal exposure to cyclopamine inhibited the occurrence of preneoplastic MB lesions and small MBs in Ptch1 mice up to 1 week after the treatment period. Concurrently, the reduction in the total area of proliferative lesions in the cyclopamine group indicated that cyclopamine treatment inhibited not only the development of preneoplastic lesions but also the expansion of these lesions. Furthermore, the inhibitory potential persisted for 2 months after treatment.

During normal cerebellar development, Shh is an important signal that regulates GCP proliferation in the EGL (Haldipur et al. 2012; Lewis et al. 2004; Vaillant and Monard 2009; Wallace 1999). GCPs express Ptch1, the receptor for Shh, and proliferate in response to Shh secreted by the Purkinje cells (Haldipur et al. 2012; Lewis et al. 2004; Vaillant and Monard 2009). Examination of the cerebellum at the peak period of GCP proliferation, PND7, provided evidence that the inhibitory effect of cyclopamine on GCP proliferation might be related to the thinning of the EGL, a place of occurrence of preneoplastic cells of MBs, in wild-type and Ptch1 mice. Immunohistochemistry indicated that thinning of the EGL was associated with decreased proliferative activity rather than increased apoptosis of GCPs by cyclopamine. In this study, at PND7, the outcome of GCPs treated with cyclopamine was consistent with GCPs treated with neutralizing anti-Shh antibodies in neonatal mice (Wallace 1999). It is known that cyclopamine inhibits the growth of cultured MB cells and allografts by inhibiting Smo (Berman et al. 2002; Dahmane et al. 2001). Furthermore, it has been reported that cyclopamine treatment inhibited MB growth *in vivo* using $Ptc1^{-/-}/p53^{-/-}$ mice and genetically engineered mice overexpressing hepatocyte growth factor (HGF) and Shh by inducing a potent apoptotic death response in tumor cells and by a suppressive effect on proliferation (Coon et al. 2010; Sanchez and Ruiz i Altaba 2005). In addition, another Smo-binding antagonist, HhAntag, completely eliminated MBs by blocking tumor cell proliferation and stimulating apoptosis (Gupta, Takebe, and Lorusso 2010; Romer et al. 2004). Taken together, the decreased proliferative activity observed in cyclopamine-treated mice in this study is thought to be attributed to the inhibition of Smo and downstream signals. Since Ptch1 haploinsufficiency alone is considered to be insufficient for tumor induction, additional genetic lesions are required for tumorigenesis (Wetmore, Eberhart, and Curran 2000; Corcoran and Scott 2001). Our data suggest that cyclopamine treatment during cerebellar development reduced production of cells that will give rise to MBs and the subsequent chances for additional mutations to occur in those cells, by decreasing proliferation of GCPs and preneoplastic cells.

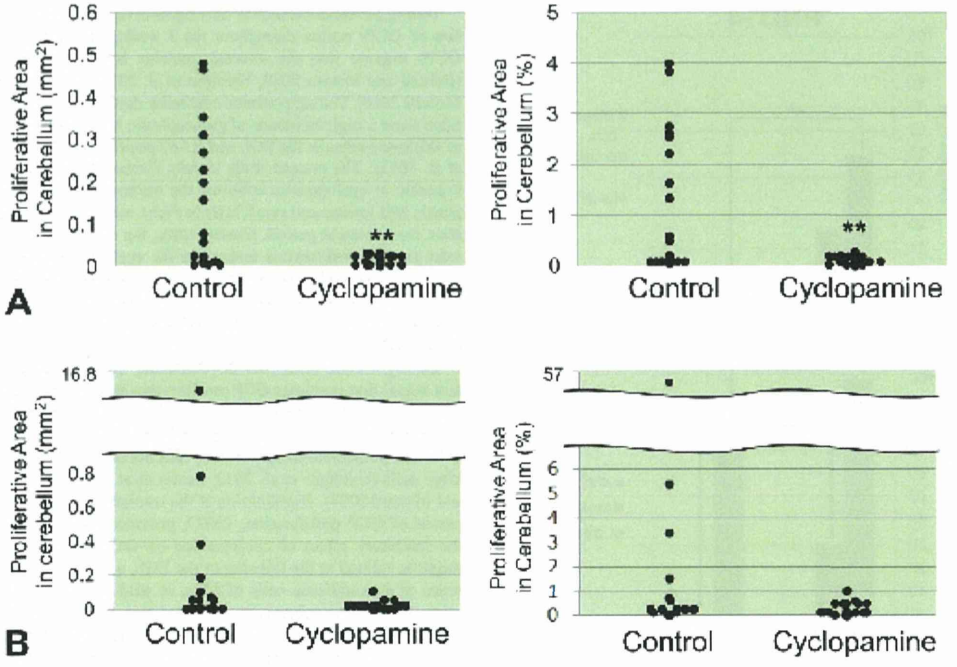

FIGURE 4.—Total area of proliferative lesions in the cerebellum of control and cyclopamine-treated Ptch1 mice at PND21 (A) and W12 (B). The total area of the proliferative lesions was calculated for each animal as the sum of areas of the Ki-67 positive foci and MBs observed in a cerebellum slide stained for Ki-67. **Significantly different from the control group; $p < .01$.
Note. PND = postnatal day; W12 = postnatal week 12; Ptch1 = patched1; MB = medulloblastoma.

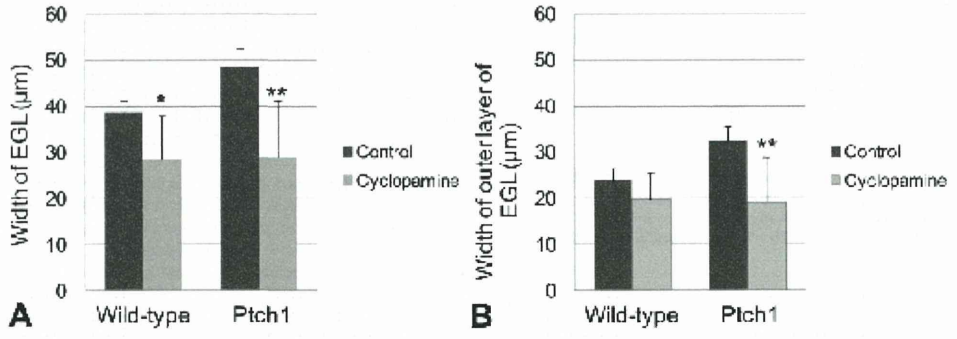

FIGURE 5.—The width of the EGL (A) and the outer layer of the EGL (B) of control and cyclopamine-treated Ptch1 and wild-type mice at PND7. *, **Significantly different from the control group at $p < .05$ and $p < .01$, respectively.
Note. PND = postnatal day; Ptch1 = patched1; EGL = external granular layer.

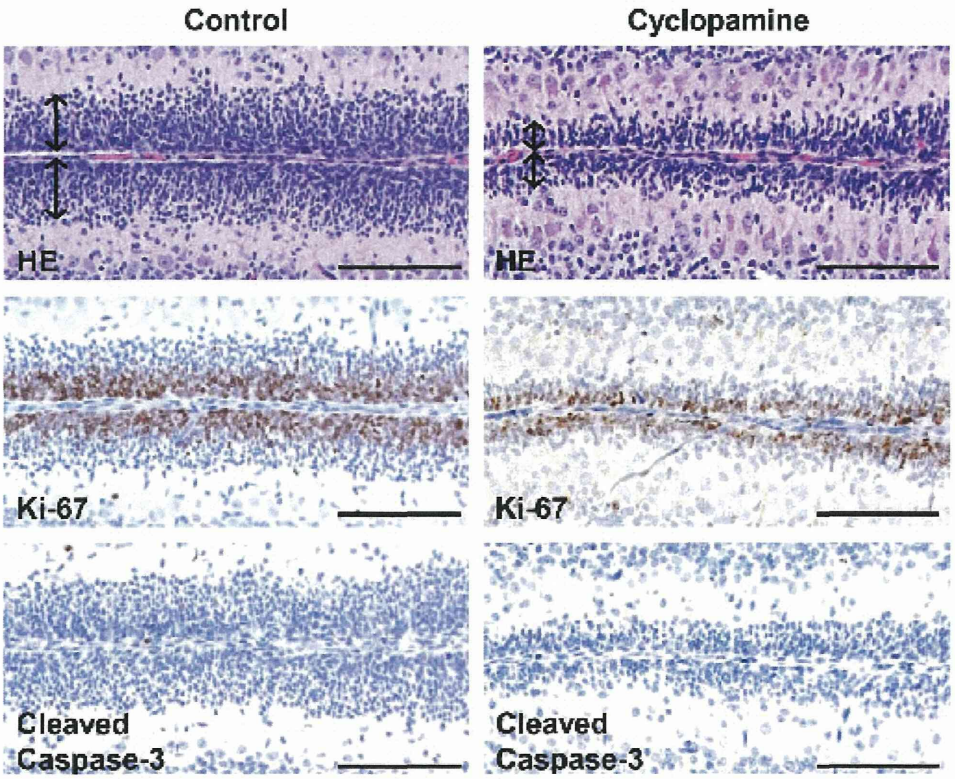

FIGURE 6.—Histopathology of the cerebellum of control (left column) and cyclopamine-treated (right column) Ptch1 mice at PND7. The EGL (arrows) was thinned in the cyclopamine group (HE, top of right column). Thinning of the Ki-67 positive layer in the EGL was also observed in the cyclopamine group (Ki-67 staining, middle of right column). There was no difference in the number of apoptotic cells in the EGL of the cyclopamine group (cleaved caspase-3 staining, bottom of right column) compared to controls. Scale bar: 100 µm.
Note. PND = postnatal day; Ptch1 = patched1; EGL = external granular layer; HE = hematoxylin and eosin.

Cerebellum volume dramatically increases during neonatal development (Lewis et al. 2004). This increase in size is predominantly due to rapid proliferation and expansion of granular cells, which are the most abundant neuronal population in the mature brain (Lewis et al. 2004). In addition, it is known that Shh is required for proliferation of precursor cells of the cerebral neocortex and tectum in postnatal mice in addition to the cerebellum (Dahmane et al. 2001; Steeca and Ruiz i Altaba 2002). Therefore, the decrease in cerebellum weight in the cyclopamine-treated group was considered to be a result of the decreased proliferation of GCPs in the EGL. Furthermore, this suggests that inhibition of Shh signaling by cyclopamine has a similar effect on postnatal cerebral development, as it does on cerebellar development and causes a decrease in overall brain weight.

NeuN-positive granular cells in the deep molecular layer of the cyclopamine-treated group may undergo precocious maturation during their migration to the internal granular layer. Abnormal Purkinje cells similar to those observed in this study have also been reported in Shh-deficient mice and were thought to be a secondary effect due to loss of GCPs (Lewis et al. 2004). In our study, the thinning of the EGL, the presence of ectopic NeuN-positive granular cells, and the misalignment of Purkinje cells are all thought to be caused by cyclopamine treatment and are related to each other because these lesions shared a common location in the cerebellum. Also, the presence of these lesions at W12 indicated that the effects of cyclopamine persisted after the completion of cerebellar development.

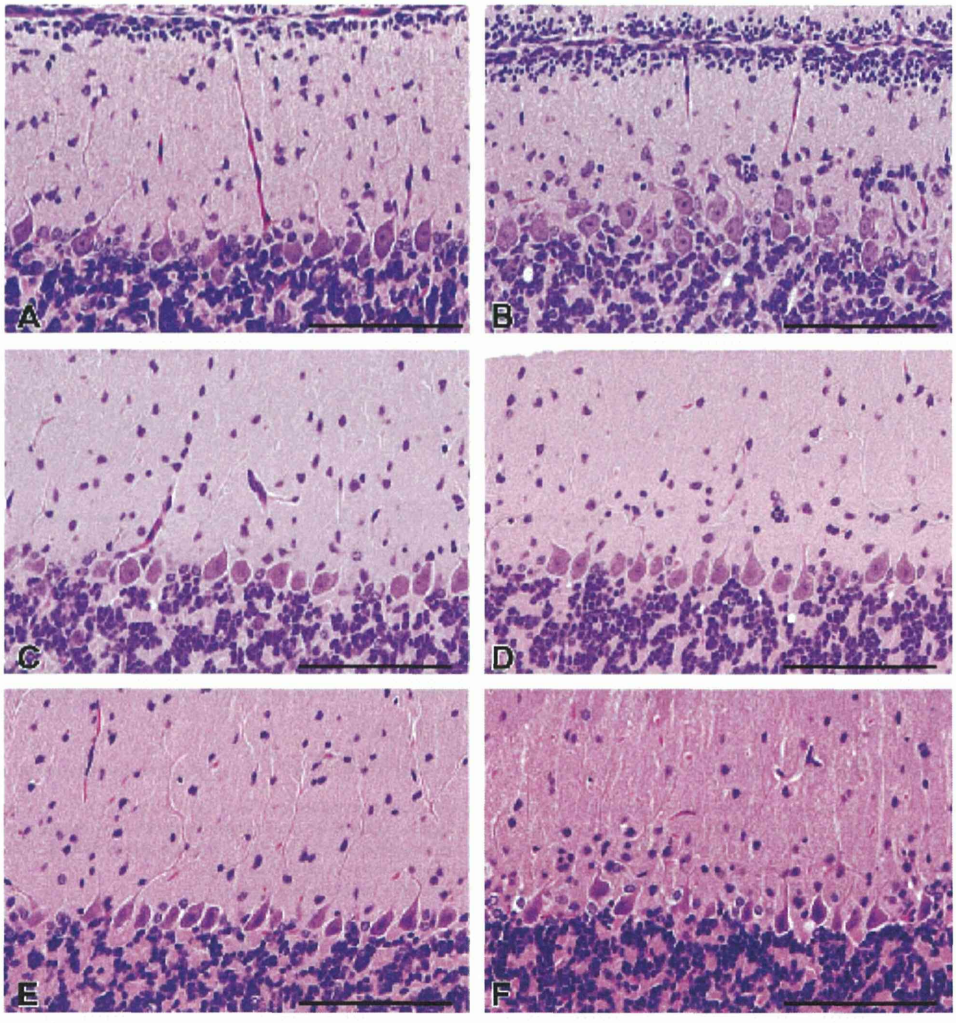

FIGURE 7.—Histopathological findings observed in the molecular layer of the cerebellum from control (left column) and cyclopamine-treated (right column) Ptch1 mice at PND14 (A and B), 21 (C and D), and W12 (E and F) (HE). Granular cells, which resemble cells of the internal granular layer, were distributed parallel to the Purkinje cell layer in the deeper molecular layer of cyclopamine-treated Ptch1 mice at PND14 (B), 21 (D), and W12 (F). Scale bar: 100 μm.
Note. PND = postnatal day; W12 = postnatal week 12; Ptch1 = patched1; HE = hematoxylin and eosin.

Whereas our previous study revealed that more than half of the Ki-67-positive foci and small MBs were located in lobules 6 through 10 of the cerebellum (Matsuo et al. 2013), in the present study the inhibitory effect of cyclopamine was observed mainly in lobules 2 through 4/5 of the cerebellum at PND7. The differences in regions that were highly affected by cyclopamine treatment during the developmental period and the common site of MB